RSC Advances

ROYAL SOCIETY OF CHEMISTRY

www.rsc.org/advances

RSC Advances

Cite this: DOI: 10.1039/c0xx00000x

www.rsc.org/xxxxxx

Paper

Fast and Facile Fabrication of Porous Polymer Particles Via Thiol-ene Suspension Photopolymerization

Jiaojun Tan, Chunmei Li, Jian Zhou, Changjie Yin, Baoliang Zhang, Junwei Gu and Qiuyu Zhang*

Received (in XXX, XXX) Xth XXXXXXXXX 20XX, Accepted Xth XXXXXXXXX 20XX

DOI: 10.1039/b000000x

A fast and facile method of preparing porous polymer particles via thiol-ene suspension photopolymerization was studied. The porous particles were fabricated by adding the porogen to the click chemistry system. In this paper, the photopolymerization of dipentaerythritol hexakis (3-mercaptopropionate), pentaerythritol tetrakis (3-mercaptopropionate), 1,3,5-tri-2-propenyl-1,3,5-triazine-2,4,6(1H,3H,5H)-trione, sodium dodecyl sulfate, chloroform and different amount of linear polymer porogen (Polymethyl methacrylate, PMMA) was discussed in detail. The two crucial factors, polymerization time and amount of porogen, were investigated. It was demonstrated that the conversion of monomers could reach 80% within 15 s of irradiation, which further vertified the high efficiency of click chemistry. By varying the amount of PMMA, we were able to tailor the particle size, pore diameters and morphology of the porous particles. Results of the mercury porosimetry indicated the median pore diameter of particles was about 12.39 μm and the surface area was 4.393 $m^2 g^{-1}$. Moreover, the T_g of the particles given by DSC was about 45℃.

Introduction

Porous polymer particles have received great research interest due to porous nature and high crosslinking degree which differentiate them from gel-type polymer particles[1], resulting in various characteristics, such as high surface area, easy incorporation of functional groups, low density and increased brittleness[2-4]. Based on these properties, porous polymer particles can be applied in many fields of ion-exchange[5], catalysis[6, 7], solid phase extraction[8, 9], drug delivery system[10], and so on.

The promising applications of porous polymer particles drive researchers to develop multiple preparation routes in decades, including suspension polymerizations[11], precipitation polymerizations[12], dispersion polymerizations[13] and high internal phase emulsions technique[14]. However, all the above methods have a common drawback at which the monomers used are acrylics and styrene ones. The polymerization of these monomers follows a chain-growth mechanism and can be hindered by oxygen and moisture, which makes the fabrication process time-consuming and energy-consuming. Thereby, to develop facile and efficient methods is an important goal to achieve.

Though thiol-ene chemistry has been known for ages, it has recently gained attention due to its click characteristics[15, 16]. Different from traditional radical system, thiol-ene click chemistry reaction follows a step-growth mechanism, and its main advantages cover extremely rapid reaction, tolerance of1 oxygen and moisture, mild reaction conditions and high-yielding[17]. As we all know, thiol-ene polymerizations have been used regularly for industrial fields via bulk polymerizations. However, preparing particles using water-borne thiol-ene click chemistry is a new field where there are only a few papers and the researchers mainly focused on using the microfluidics to fabricate particles. Prasath fabricated macroporous and nonporous functional polymer beads via click chemistry in microfluidics and investigated influence of the variety of monomers[18]. In their work, the uniform and functional polymer particles have been prepared, however, special microfluidic device was difficult to achieve. Khutoryanskiy applied thiol-ene click reactions with non-stoichiometric ratio for the synthesis of thiol- and acrylate-functionalized nanoparticles, and the unreacted groups on the surface of particles provide materials with mucoadhesive properties[19]. Durham prepared polymer microspheres via water-borne thiol-ene suspension photopolymerization, which offered great potential of developing thiol-ene microspheres with high monomer conversions, rapid reaction rates and uniform cross-link density, etc[20].

* *Department of Applied Chemistry, School of Science, Northwestern Polytechnical University, Youyi Road 127#, Xi'an, China.*
Fax: +86-029-88431653; tel: +86-029-88431675;
E-mail: qyzhang1803@gmail.com

Based on the aforementioned research, we herein report a thiol-ene suspension photopolymerization to prepare porous polymer particles using a simple procedure under mild reaction conditions. In particular, the remarkable advantage of this method is efficient and high yield. In this work, the step-growth mechanism was incorporated to water-borne suspension polymerization, and this was the first combination of porogen and thiol-ene click chemistry to fabricate porous particles, to our knowledge. Moreover, particle morphology and size can be effectively controlled depending by varying two crucial factors, polymerization time and porogen amount.

Materials and Methods

Materials

Methyl methacrylate (MMA, AR, Tianjin Hongyan Chemical Reagents Factory) was kept in refrigerator. Pentaerythritol tetrakis (3-mercaptopropionate) (PETMP, >90%), 1-hydroxycyclohexyl phenyl ketone (Iragcure 184, GC) and 1,3,5-Tri-2-propenyl-1,3,5-triazine-2,4,6(1H,3H,5H)-trione (TATATO, GC) were all obtained from TCI Chemical Reagent Co., Ltd. Dipentaerythritol hexakis(3-mercaptopropionate) (DPMP, CP) was purchased from Guangzhou Sgsmt Special Materials Technology Co. Ltd. Sodium dodecyl sulfate (SDS, CP) was purchased from Sinopharm Chemical Reagent Co.,Ltd. All the above chemical reagents were used without further purification. 2,2'-Azobis(2-methylpropionitrile) (AIBN, CP, Energy Chemical) was recrystallized in ethanol before use. The water used throughout this experiment was produced by our lab.

UV lamp (Lightningcure L8868) was purchased from Hamamatsu, Japan. The radiant wavelength range from 300 nm to 450 nm, and the intensity, detected using a UV light radiometer (UV-INT 150, Germany), was about 18 mW cm^{-2} based on keeping 1 cm irradiation distance and 100% output light intensity.

Synthesis of linear polymer porogen

PMMA was selected as the linear polymer porogen and synthesized by solution polymerization as follows. MMA (0.2 mol, 20 g) and AIBN (1.2 mmol, 0.2 g) were dissolved in 60 mL toluene in a 100 mL round bottom flask fitted with a mechanical stirrer and condenser, then the reaction mixture was heated to 80 ℃ and kept for 6 h under stirring. The number average molecular weight (Mn) and molecular weight distributions (PDI) of the obtained PMMA were 27279 g mol^{-1} and 1.897, respectively.

Fabrication of porous polymer particles

The porous polymer particles were synthesized by suspension polymerization. The polymerization was carried out in a 50 mL beaker equipped with a mechanical stirrer. In a typical procedure, aqueous phase was obtained via dissolving 1.0 g SDS in 20.0 g H_2O. And then, Iragcure 184 (0.02 g) was dissolved in a mixture of PETMP (2 mmol, 0.976 g), DPMP (0.33 mmol, 0.261 g), TATATO (3.3 mmol, 0.833 g), $CHCl_3$ (2.0 g) and various amount of porogen (seen in table 1) in a 10 mL beaker that was covered with a piece of aluminum foil to avoid light penetration. The uniform and transparent mixture was obtained after ultrasonic treatment for ten minutes. Then, the mixture was introduced into aqueous phase at room temperature with a stirring rate of 400 rpm and the emulsification procedure was kept for 5 min. Subsequently, thiol-ene photopolymerization was irradiated at room temperature under continuous UV light which was generated by a UV spot source (Lightningcure L8868, Hamamatsu, Japan). After photopolymerization, the resulting particles were purified to remove porogen by repeating three cycles of centrifugation-washing-redispersion using water and ethanol, respectively.

Table 1 Amount of PMMA (weight ratio of the total monomers) used in the preparations

Sample	A	B	C	D	E
Amount	0	10%	20%	30%	40%

Characterization

The real-time FTIR spectra to monitor thiol-ene photopolymerization process was recorded by a Bruker Tensor 27 Fourier transform infrared spectroscope. The detailed information of operation method and mechanism was refered to Zhou[21]. Differential scanning calorimetry (DSC) was performed on a differential scanning calorimeter (DSC2910, TA Instruments), with a heating rate of 10 ℃ min^{-1} between -20 ℃ and 120 ℃. The morphologies of polymer particles were characterized by a Scanning Electron Microscope (SEM, JEOL JSM-6700F). An accelerating voltage of 10 kV with an Au coating of the sample was used to image these particles. The pore properties of porous polymer spheres were measured by mercury porosimetry (AUTOPORE IV 9500, Micromeritics, USA). Molecular weights and molecular weight distributions were determined by gel permeation chromatography (GPC) equipped with a Waters 1515 pump and a Waters 2414 differential refractive index detector (set at 30 ℃). The eluent was DMF at a flow rate of 1.0 mL min^{-1}. Monodispersed polystyrene standards were used to obtain a calibration curve. The average diameter and particle size distribution of the porous particles were determined by LS13320 Laser Particle Size Analyzer (Beckman Coulter). Yield of particles was calculated by Equ. 1.

$$\text{Yield} = m_1/m_2 \times 100\% \quad (1)$$

Where m_1 and m_2 are the mass of obtained particles and total monomers, respectively.

Results and discussion

Influence of photopolymerization time

For obtaining the excellent properties, high monomer conversion should be guaranteed, thus polymerization time is a vital factor that controls the properties of polymer particles prepared via suspension polymerization. In traditional radical system, polymerization process takes several hours due to inhibition of oxygen and moisture. Excitingly, thiol-ene photopolymerization is an efficient method which could reach high monomer conversion within several seconds. In order to make full use of advantages of thiol-ene system, it is necessary to determine an appropriate polymerization time. As we know, every single monomer droplet in suspension polymerization behaves like a microreactor of bulk polymerization[1]. Therefore, polymerization kinetics of thiol-ene bulk polymerization can be monitored via real-time FTIR and expanded to suspension polymerization.

The characteristic absorbance bands used to monitor the disappearance of the reactant during the photopolymerization were thiol (2570 cm^{-1}) and allyl (3080 cm^{-1}), and the conversion was calculated from the change of corresponding peak area. Fig. 1a showed the infrared spectral changes of the thiol and allyl groups as the reaction proceeded. The infrared spectrum areas significantly reduced after 5 s of irradiation, and changed little after 130 s of irradiation. Meanwhile, the area decreased most in the first five seconds, and the decrease speed of area slowed down with time. Fig. 1b depicted the conversion of thiol and allyl groups as a function of irradiation time. It could be seen from Fig. 1b that the conversions of thiol and allyl groups increased very rapidly and reached 80% after irradiation for 15 s. It was evident that the conversion of allyl was higher than thiol, and the ultimate conversion of thiol and allyl reached 88% and 93%, respectively. The higher conversion of allyl was ascribe to the homopolymerization of a part of allyl(~5%)[15].

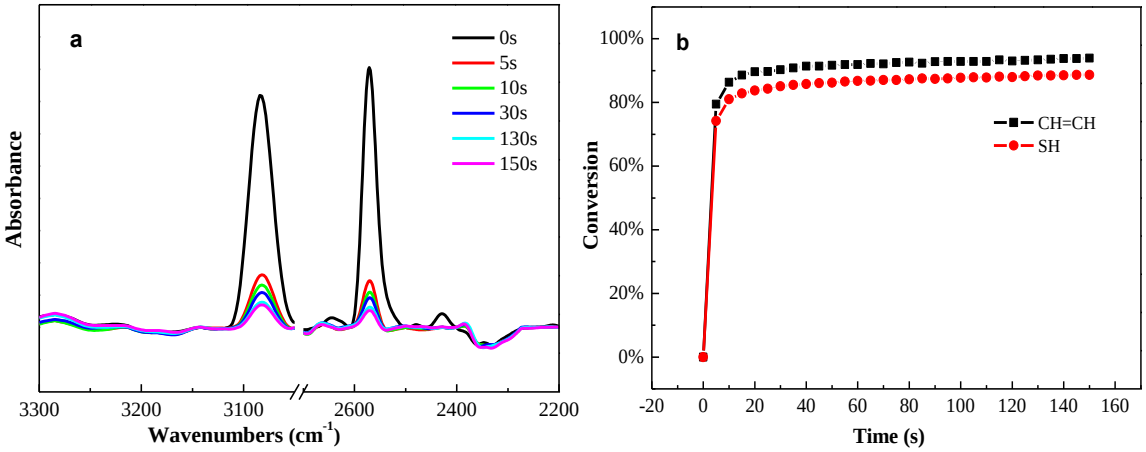

Fig. 1 (a) Real-time FTIR spectra (b) FTIR conversions of allyl and thiol groups as a function of irradiation time with a UV irradiance of 18 mW cm^{-2}. The bulk polymerization recipe was similar with sample A.

The morphology of particles under different irradiation time was shown in Fig. 2, and the formulation was the same as sample A. It was evident from Fig. 2 that the surface was quite smooth after 30 s of irradiation, and changed little with irradiation time increased. Further research verified that increasing irradiation time could improve yield. Fig. 3 depicted yield of particles as a function of irradiation time. From Fig. 3, the ultimate yield of particles was approximately 75% within 300s. The reason why yield increasing with time was as follows, although thiol-ene chemistry was fast and efficient, only those droplets exposed to UV formed particles in suspension system. The other droplets were still monomer droplets and washed away by alcohol in the process of particle purification, so increasing irradiation time was equal to increase the opportunity of droplet exposure to UV. In conclusion, the optimum polymerization time was set at 300 s, which could achieve the best balance among particles' surface, yield and polymerization effiency.

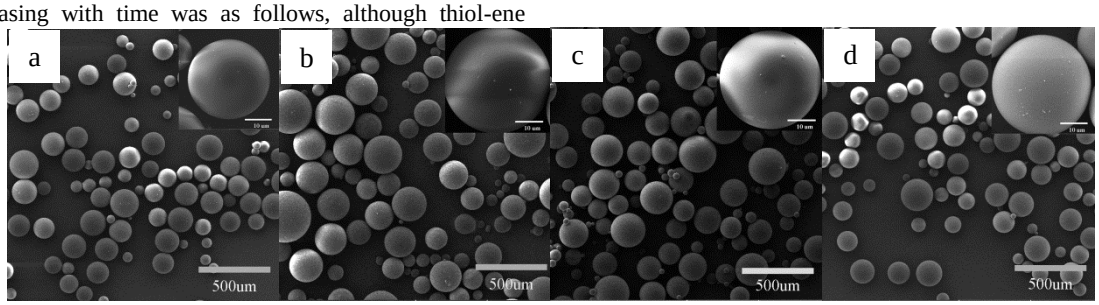

Fig. 2 SEM images of the particle morphology with the different polymerization time. a. 30 s, b. 1min, c. 5min and d. 15min (The scale bar of the insert image was 10μm)

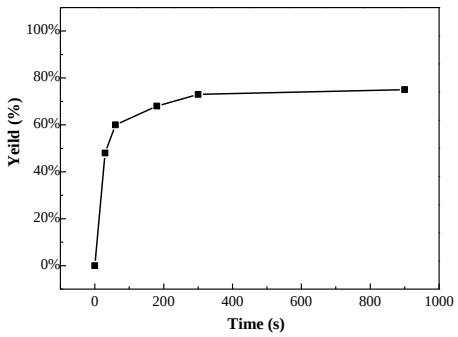

Fig. 3 Yield of particles as a function of irradiation time

Influence of porogen

The amount of porogen has a significant effect on the pore of the particles, because it not only affects pore size, volume and distribution, but also adjusts particle sizes via changing viscosity of the organic phase. Hence, it's necessary to investigate the effect of porogen on morphology and particles size.

Fig. 4 showed the effect of linear polymer porogen (PMMA) amount on porous particle morphology. As we can see from Fig. 4, the surface is smooth when the amount of PMMA was little, and the porous structure became more apparent with increasing the PMMA amount. Meanwhile, the particle diameters increased, which was because of the increased viscosity when more PMMA

added. Moreover, it was clear that PMMA played an important role in the pore formation, and large pores are formed with increasing the amount of PMMA. The cross-section SEM image of the porous particles was presented in Fig. 5. And likewise, macroporous structure was evident inside the porous particles. The reason for formation of macrospores was that pore formation occurs via χ-induced syneresis. Pore formation followed this mechanism in most cases when nonsolvent or linear polymer was used as porogen. In this case, they cannot swell or dissolve the growing chains because of poor compatibility, and phase separation occurred before the gelation point. The first separated polymer particles acted as nuclei and grew as a discontinuous phase inside every discrete monomer droplet, and the growing partilces agglomerated to form the porous particles finally[1]. As a result, the main characteristics of particles following this mechanism were large pores size and low surface area. However, the porous particles couldn't be formed when the amount of porogen exceeded a critical point. When the PMMA was more than 50% in our experiment, the porous particles couldn't be formed, which was because the reactive polymer could not form a continuous phase or the strength of polymer was poor to form particles.

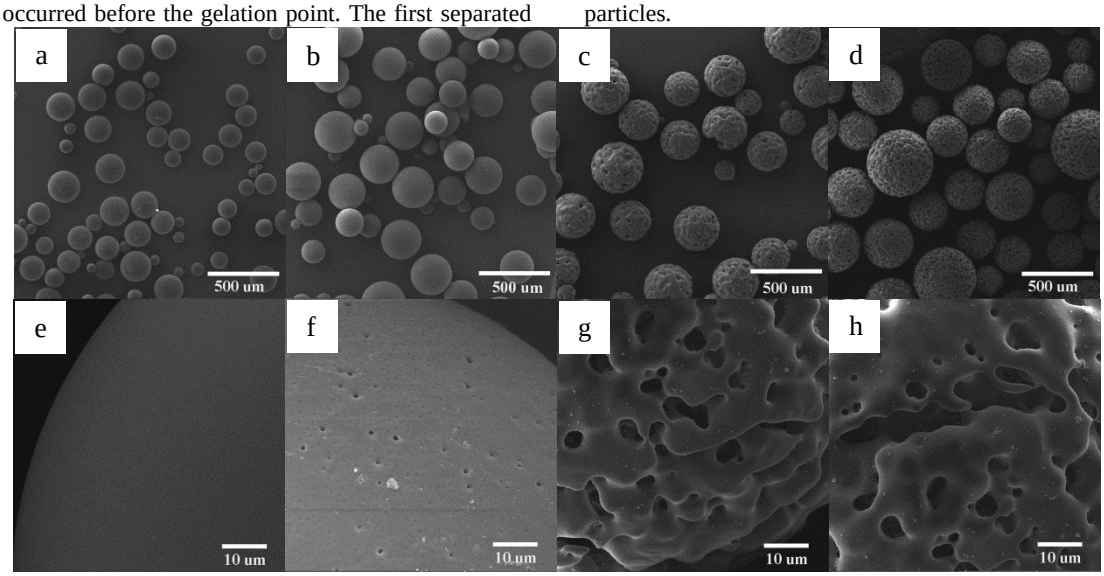

Fig. 4 The full view SEM images of particle morphology with various PMMA amount: (a) sample B, (b) sample C, (c) sample D and (d) sample E , respectively; and their corresponding surface SEM images (e), (f), (g) and (h)

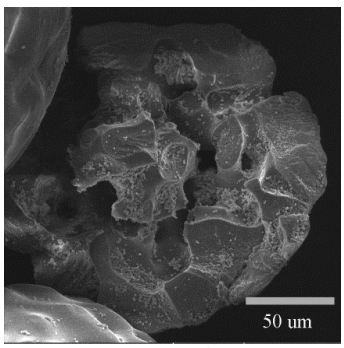

Fig. 5 The cross-section SEM images of the porous particles(Sample E)

Fig.6 depicted the effect of PMMA amount on particle diameter and distribution. The average particle diameter increased with the amount of porogens increasing and highercontent of porogen resulted in larger polymer particles and wider particle size distributions. This phenomenon was determined by the viscosity of organic phase and the mechanism of suspension polymerization. First, microdroplets were created by mechanical agitation, and then droplets were cured to form microspheres in the presence of UV. Since droplet collision and break-up took place throughout the whole process, and high viscous organic phase made droplet's break-up difficult to occur, which disturbed the balance of collision and break-up.

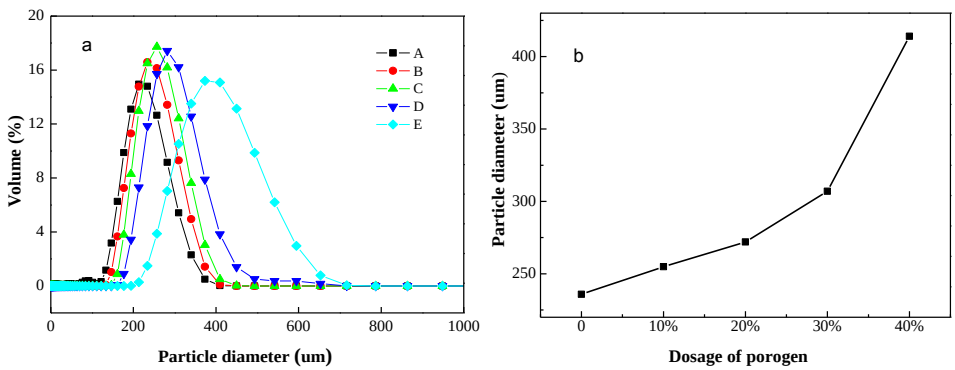

Fig.6 (a) The particle size distributions and (b) the mean particle size as a function of the PMMA amount**.**

Pore properties of porous polymer particles

The porous morphology of sample E was the most representative among these particles, so we took it as an example to investigate pore properties. Pore size distribution of particles was characterized by the mercury porosimetry as depicted in Fig.7, and the detailed information of porous particles was listed in table 2. The results, presented in table 2, showed that the surface area was only 4.393 m^2 g^{-1} and porosity could reach 57%. This was attributed to the aforementioned χ-induced syneresis mechanism that phase separation occurred early in polymerization and the resulting particles had a large pore volume, relatively low surface area and large pore size. This phenomenon was similar to macroporous GMA- EDMA particles using PMMA as porogen, whose pore volume was up to 1.5 mL g^{-1} and surface area less than 10 m^2 g^{-1}.[22] It was evident from Fig.6 that the pores were mainly on the micrometer scale, and the diameter of predominant macropores was about 12.39 μm which was in accordance with Fig. 4.

Table2 The pore property of sample E measured by mercury intrusion porosimetry

Total Intrusion Volume	Total Pore Area	Median Pore Diameter	Apparent Density
1.3885 mL g^{-1}	4.393 m^2 g^{-1}	12.39 μm	0.9797 g mL^{-1}

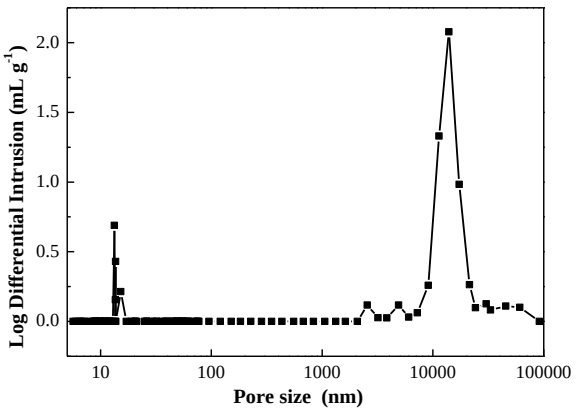

Fig. 7 Pore size distribution of sample E measured by mercury intrusion porosimetry

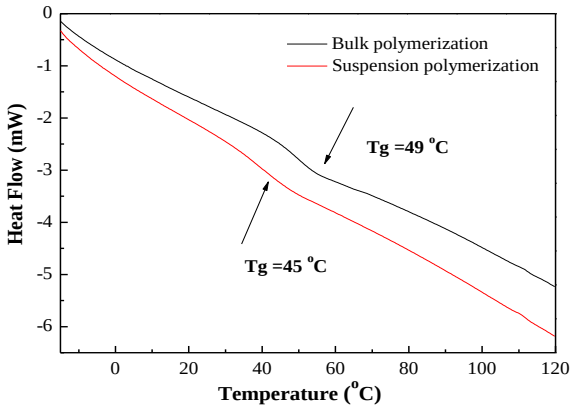

Fig. 8 The DSC curve of particles obtained by suspension polymerization (sample E) and the sample of bulk polymerization

Thermal properties of porous polymer particles

In order to investigate thermal properties of the particles and further conform that there is little difference in thermal properties between suspension polymerization and bulk polymerization, the T_gs of particles were characterized by DSC. Both suspension and bulk polymerizations contained monomers and chloroform, but suspension polymerizations additionally contained water, surfactant, and 40% PMMA. Fig. 8 showed that the obtained T_gs were slightly different, and the T_gs were about 45℃ and 49℃ for suspension and bulk polymerizations, respectively. This phenomenon further confirmed aforementioned mechanism, that is every single monomer droplet in suspension polymerization behaved like a microreactor of bulk polymerization, and the composition and network structure of suspension and bulk polymerization were almost the same. Compared with Krishnan's work[20], T_g of particles increased by 40℃ after introducing DPMP, which significantly improved the strength of particles. This was attributed to that DPMP increased monomer functionality and system crosslinking density, thus enlarged the potential service temperature.

Conclusion

In conclusion, porous polymer particles have been fabricated via thiol-ene suspension photopolymerization. Different from traditional methods, the process of polymerization via thiol-ene click chemistry is highly efficient, and the characteristics of the efficient and high-yielding will promote the development of porous polymer particles. We have found that the amount of PMMA has a profound effect on particles' morphology and diameter. More PMMA amount leads to coarser surface and larger particle size. DPMP could significantly improve Tg of particles, and might enlarge the potential service temperatures.

Acknowledgments

The authors are grateful for the financial support provided by National High Technology Research and Development Program of China (No. 2012AA02A404), National Natural Science Foundation of China (No. 51173146, No.51173147) and basic research fund of Northwestern Polytechnical University (JC20120248).

References

1. M. T. Gokmen and F. E. Du Prez, *Prog. Polym. Sci.*, 2012, **37**, 365-405.
2. D. Wu, F. Xu, B. Sun, R. Fu, H. He and K. Matyjaszewski, *Chem. Rev.*, 2012, **112**, 3959-4015.
3. R. Dawson, A. Laybourn, R. Clowes, Y. Z. Khimyak, D. J. Adams and A. I. Cooper, *Macromolecules*, 2009, **42**, 8809-8816.

4. B. Li, X. Huang, L. Liang and B. Tan, *J. Mater. Chem.*, 2010, **20**, 7444-7450.
5. F. S. Macintyre, D. C. Sherrington and L. Tetley, *Macromolecules*, 2006, **39**, 5381-5384.
6. L. Chen, Y. Honsho, S. Seki and D. Jiang, *J. Am. Chem. Soc.*, 2010, **132**, 6742-6748.
7. L. Jinhua, L. Dongliang, W. Honghua and Z. Guangyuan, *Polymer*, 2011, **52**, 602-605.
8. D. Bratkowska, N. Fontanals, F. Borrull, P. Cormack, D. Sherrington and R. Marcé, *J. Chromatogr. A*, 2010, **1217**, 3238-3243.
9. F. Barahona, E. Turiel, P. A. Cormack and A. Martín‐Esteban, *J. Sep. Sci.*, 2011, **34**, 217-224.
10. S. Freiberg and X. Zhu, *Int. J. Pharm.*, 2004, **282**, 1-18.
11. F. S. Macintyre and D. C. Sherrington, *Macromolecules*, 2004, **37**, 7628-7636.
12. W. H. Li and H. D. Stöver, *J. Polym. Sci., Part A: Polym. Chem.*, 1998, **36**, 1543-1551.
13. A. Moustafa, T. Kahil and A. Faizalla, *J. Appl. Polym. Sci.*, 2000, **76**, 594-601.
14. A. Menner, R. Verdejo, M. Shaffer and A. Bismarck, *Langmuir*, 2007, **23**, 2398-2403.
15. N. B. Cramer and C. N. Bowman, *J. Polym. Sci., Part A: Polym. Chem.*, 2001, **39**, 3311-3319.
16. M. J. Kade, D. J. Burke and C. J. Hawker, *J. Polym. Sci., Part A: Polym. Chem.*, 2010, **48**, 743-750.
17. J. W. Chan, C. E. Hoyle and A. B. Lowe, *J. Am. Chem. Soc.*, 2009, **131**, 5751-5753.
18. R. A. Prasath, M. T. Gokmen, P. Espeel and F. E. Du Prez, *Polymer Chemistry*, 2010, **1**, 685-692.
19. A. Storha, E. A. Mun and V. Khutoryanskiy, *RSC Adv.*, 2013, **3**, 12275–12279.
20. O. Z. Durham, S. Krishnan and D. A. Shipp, *ACS Macro Letters*, 2012, **1**, 1134-1137.
21. J. Zhou, Q.-y. Zhang, S.-j. Chen, H.-p. Zhang, A.-j. Ma, M.-l. Ma, Q. Liu and J.-j. Tan, *Polym. Test.*, 2013, 608– 616.
22. D. HORAK, J. LABSKY, J. PILAR, M. BLEHA, Z. PELZBAUER and F. SVEC, *Polymer*, 1993, **34**, 3481-3489.

A table of contents entry

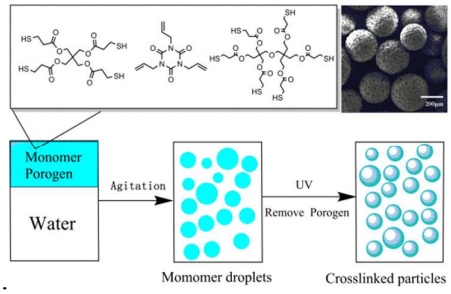

The porous particles were fabricated via thiol-ene click chemistry within 5 minutes under mild conditions.